

Article

# High Bio-Content Thermoplastic Polyurethanes from Azelaic Acid

Bhausahab S. Rajput, Thien An Phung Hai and Michael D. Burkart \* 

Department of Chemistry and Biochemistry, University of California, San Diego, 9500 Gilman Dr., La Jolla, CA 92093-0358, USA; bsrajput@ucsd.edu (B.S.R.); h1phung@ucsd.edu (T.A.P.H.)

\* Correspondence: mburkart@ucsd.edu

**Abstract:** To realize the commercialization of sustainable materials, new polymers must be generated and systematically evaluated for material characteristics and end-of-life treatment. Polyester polyols made from renewable monomers have found limited adoption in thermoplastic polyurethane (TPU) applications, and their broad adoption in manufacturing may be possible with a more detailed understanding of their structure and properties. To this end, we prepared a series of bio-based crystalline and amorphous polyester polyols utilizing azelaic acid and varying branched or non-branched diols. The prepared polyols showed viscosities in the range of 504–781 cP at 70 °C, with resulting TPUs that displayed excellent thermal and mechanical properties. TPUs prepared from crystalline azelate polyester polyol exhibited excellent mechanical properties compared to TPUs prepared from amorphous polyols. These were used to demonstrate prototype products, such as watch bands and cup-shaped forms. Importantly, the prepared TPUs had up to 85% bio-carbon content. Studies such as these will be important for the development of renewable materials that display mechanical properties suitable for commercially viable, sustainable products.

**Keywords:** bio-carbon content; polyester polyols; thermoplastic polyurethanes; prototyping



**Citation:** Rajput, B.S.; Hai, T.A.P.; Burkart, M.D. High Bio-Content Thermoplastic Polyurethanes from Azelaic Acid. *Molecules* **2022**, *27*, 4885. <https://doi.org/10.3390/molecules27154885>

Academic Editor: Hua Wei

Received: 10 June 2022

Accepted: 26 July 2022

Published: 30 July 2022

**Publisher's Note:** MDPI stays neutral with regard to jurisdictional claims in published maps and institutional affiliations.



**Copyright:** © 2022 by the authors. Licensee MDPI, Basel, Switzerland. This article is an open access article distributed under the terms and conditions of the Creative Commons Attribution (CC BY) license (<https://creativecommons.org/licenses/by/4.0/>).

## 1. Introduction

The field of renewable and biodegradable polymers is rapidly growing and attracting significant attention due to pressing environmental concerns [1–8]. Renewable feedstocks will play an important role in reducing greenhouse gas emissions and ensuring energy security in the 21st century [7,9,10]. Progressively increasing the renewable feedstock content of chemicals and materials will help create the mass markets for renewable feedstocks required to bring down their costs to make them competitive with petroleum sources [11]. The utilization of bio-based materials for product prototypes is a precondition to competing in the marketplace and represents a first step that can be met by material scientists. Thermoplastic polyurethanes (TPUs) are among the most versatile and broadly adopted materials used in applications such as shoes, industrial belts, sporting goods, medical devices, cabling, golf balls, cellular phone covers, watch bands, and automobile interiors. TPUs are segmented linear block copolymers formed by reaction of alternating soft segments (polyols) and hard segments (made from reaction of chain extenders and isocyanates) [12]. TPUs attract substantial interest because they possess many useful properties, including mechanical strength, modifiable flexibility, good abrasion resistance, elasticity, and transparency [12]. Depending on the structure of the polyol and isocyanate during synthesis, this material can present properties that range from soft elastomers to hard plastics [13]. Most TPU products are made from petroleum-based chemicals, and utilizing bio-based ingredients for the development of high-performance TPUs is a major focus of current polyurethane research.

Dicarboxylic acids obtained from biological sources are important biomass-derived chemicals that are used for many monomers and industrial chemical intermediates [14]. As

a result, it is projected that bio-derived carboxylic acids can be made economically viable, and may result in the development of disruptive bio-based aliphatic polyesters. Dicarboxylic acids are one of the main ingredients for making polyester polyols for polyurethane applications and are key building blocks for TPUs. Recently, aliphatic polyesters from bio-derived carboxylic acids have been explored for use in renewable TPUs [15–17]. Given that we can source azelaic acid from microalgae, the most sustainable photosynthetic biomass, we have focused our attention on developing polyurethanes from this monomer [18].

In a recent study of TPUs made from azelate polyols, it was shown that even-numbered methylene repeat units from n-alkanediols can result in desirable physical properties [19]. The combination of bio-based azelaic acid with succinic and adipic acids for the synthesis of co-monomeric polyester polyol soft segments has provided significant improvements in dynamic properties of TPUs [20]. A comparison between petroleum-based adipic versus renewable azelaic acid polyester polyols as building blocks for soft TPUs indicated a slightly higher degree of phase separation for azelate compared to analogous adipate polyols [16]. A study on structure–property relationships for crystalline and amorphous azelate polyols, and their effect on TPU properties, found that TPUs based on crystalline azelate polyols have higher material strength compared to amorphous azelate polyol-based TPUs [17]. In another report, the authors prepared segmented thermoplastic polyurethanes from various molecular weight polyester polyols with 1,6-hexamethylene diisocyanate (6HDI) and 1,3-propanediol (1,3-PDO) and investigated the degree of microphase separation [21]. To date, most of these TPUs have been prepared from aromatic diisocyanate (4,4'-MDI), and there is no report on the utilization of aliphatic diisocyanates, such as 1,6-hexamethylene diisocyanate (6HDI) with bio-based azelate polyester polyols, for the preparation of TPUs. Similarly, no studies have reported the effect of amorphous azelate polyols incorporated with 2-methyl 1,3-propanediol (2MPDO), and 3-methyl 1,5-pentanediol (3MPDO) branched-chain diols on the structural and functional property relationship of TPUs.

Here, we explore the effect of two diols, 2MPDO, and bio-based 3MPDO, incorporated into amorphous azelate polyols and compare these with 1,3-propanediol-based crystalline azelate polyol. We demonstrate the usefulness of amorphous TPUs for prototype applications.

## 2. Results and Discussions

### 2.1. Polyester Polyol Synthesis

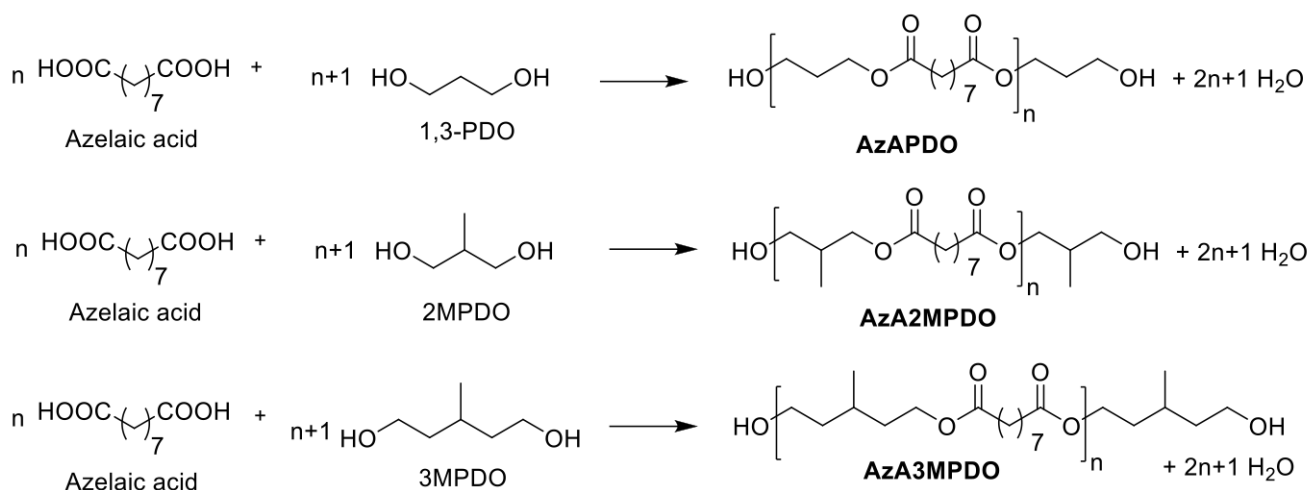
In the present study, bio-based azelate polyester polyols were synthesized from commercial azelaic acid and various branched and non-branched diols, including 1,3-propanediol, 2-methyl 1,3-propanediol (2MPDO), and 3-methyl 1,5-pentanediol (3MPDO), and using a dibutyltin dilaurate (DBTDL) catalyst (see Table 1 for details of the formulation). Although the combination of azelaic acid with 1,3-propanediol-based polyester polyol is well explored in the literature [17], polyester polyols based on azelaic acid in combination with 2MPDO and 3MPDO have been not reported. Here, the synthesis of polyester polyols was carried out under a nitrogen atmosphere at 160 °C, where the rapid release of water condensate was observed. The temperature was raised to 180 °C to complete the conversion of diacid and diol into polyester polyol (see Section 3 for detailed polyol synthesis and Table 1 for detailed polyol formulations). The individual polyol reactions were continued until anticipated hydroxyl and acid numbers were achieved (for instance, below 2 mg KOH/g). The formation of the resulting polyester polyols was investigated using NMR spectroscopy (Scheme 1). <sup>1</sup>H NMR of azelate polyols such as AzAPDO, AzA2MPDO, and AzA3MPDO displays a chemical shift at around  $\delta$  2.08–2.24 ppm, which matches the ester group attached methylene protons (originated from the azelaic acid backbone, respectively), while the peak at  $\delta$  3.95–4.17 ppm corresponds to the ester-attached methylene group (originated from the 1,3-PDO, 2MPDO, and 3MPDO diols backbone) (Table 2, Run 1–3; ESI Figures S1, S3, and S5, See Supplementary Materials). The structural identity of AzAPDO, AzA2MPDO, and AzA3MPDO polyols was further validated by <sup>13</sup>C NMR. Resonance at  $\delta$  173.7–174.3 ppm is the distinguishing peak of an ester carbonyl carbon in

polyester polyols (Table 2, Run 1–3; ESI Figures S2, S4 and S6). The prepared polyester polyols were subjected to viscosity analysis, and all viscosity measurements were carried out at 70 °C. Due to the structural diversity in the obtained polyester polyols, all showed variable viscosity values. For example, crystalline AzAPDO had viscosity up to 683 cP, which closely matches the reported value [17], whereas the other two amorphous polyester polyols, AzA2MPDO and AzA3MPDO, displayed viscosity values up to 781 cP and 504 cP, respectively. The increased viscosity in the case of branched AzA2MPDO polyester polyol is explained by the presence of the branched methyl group, which restricts molecular motion due to increased polymer chain slip-resistance within similar molecules. These polyol viscosity observations were supported by a study conducted by TNM Tuan Ismail and co-workers, whereby the viscosity of a polyester polyol was found to be increased with an increase in the volume of branching in the molecule [17]. The lower viscosity observed for AzA3MPDO polyester polyol is most likely due to the increased chain length of diol (3MPDO), which ultimately increased the chain length of the resultant polyester polyol and hence decreased the physical interactions, such as polar interaction between the alcohol and ester functional groups. The crystalline polyester polyol (AzAPDO) was found to be solid at room temperature (25 °C), and amorphous polyols showed a liquid form (Table 2).

**Table 1.** Polyester polyol formulations.

	Polyols	Azelaic Acid (mole)	1,3-PDO (mole)	2MPDO (mole)	3MPDO (mole)	<sup>(d)</sup> Catalyst (mole%)
01	<sup>(a)</sup> AzAPDO	2.11	2.36	-	-	0.019
02	<sup>(b)</sup> AzA2MDO	1.96	-	2.23	-	0.020
03	<sup>(c)</sup> AzA3MPDO	1.73	-	-	2.01	0.022

<sup>(a)</sup> AzA—azelaic acid, polyol made from azelaic acid and 1, 3-propanediol (1,3-PDO); <sup>(b)</sup> polyol made from azelaic acid and 2-methyl 1, 3-propanediol (2MPDO); <sup>(c)</sup> polyol made from azelaic acid and 3-methyl 1, 5-pentanediol (3MPDO); <sup>(d)</sup> DBTDL—dibutyltin dilaurate catalyst.



1, 3-PDO = 1, 3- propanediol; 2MPDO = 2-methyl 1, 3 propanediol; 3MPDO = 3-methyl 1, 5-pentanediol

**Scheme 1.** Synthesis of polyester polyols.

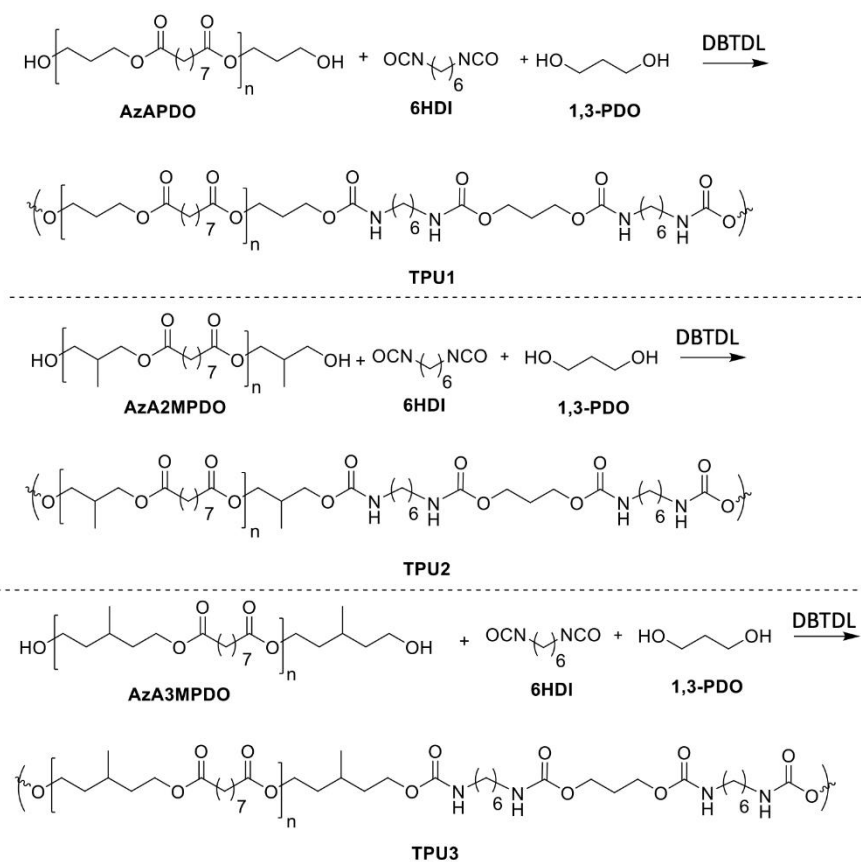
**Table 2.** Properties of polyester polyols.

Run	Polyols	Acid Value (mg KOH/g)	Hydroxyl Value (mg KOH/g)	<sup>(a)</sup> Molecular Weight (by OH Number)	<sup>(b)</sup> Viscosity (70 °C, cP)	Physical State of Polyols at (25 °C)
01	AzAPDO	1.4	56	2000	683	Solid
02	AzA2MDO	1.7	53	2100	781	Liquid
03	AzA3MPDO	1.0	57	2000	504	Liquid

<sup>(a)</sup> Molecular weight is calculated using hydroxyl number titration,  $56,000/\text{OH number} \times \text{functionality}$ ; <sup>(b)</sup> viscosity measurement was determined from the rheometer.

## 2.2. Synthesis of Thermoplastic Polyurethanes

Azelaate polyester polyols were subjected to TPU synthesis (Scheme 2). Prior to synthesis, polyols were dried in a vacuum oven at 70 °C for 24 h. TPU synthesis was performed at the low temperature of 75 °C in plastic cups using a speed mixer with an appropriate monomer ratio. Preheated polyol, chain extender (such as 1,3-PDO), and catalyst were premixed and added the preheated (at 75 °C) hexamethylene diisocyanate (6HDI), where the ratio between polyol mixture/NCO was 1/1.1 (see Table 3 for detailed formulation). The resulting mixture was poured into a Teflon dish to generate an average sheet thickness of 3–4 mm for further analysis. For real-world applications, the TPUs were also demonstrated for flexibility and toughness via a watch and plastic cup mold, as prototypes for high bio-content TPUs to replace petroleum versions (Figure 1).

**Scheme 2.** Synthesis of TPUs.

**Table 3.** Designations, chemical compositions, the molar ratio of monomers used in the preparation of TPUs, and percent bio-carbon content for TPUs.

TPUs	Chemical Compositions	Molar Ratio (Polyol:PDO:6HDI)	Hard Segment Concentration (wt %)	Bio-Carbon Content (%)
TPU1	AzAPDO, PDO, 6HDI	1:1:2.1	18.1	~85
TPU2	AzA2MPDO, PDO, 6HDI	1:1:2.1	17.4	~65
TPU3	AzA3MPDO, PDO, 6HDI	1:1:2.1	18.2	~85

**Figure 1.** Photographs of bio-based TPUs (TPU2—a cup; TPU3—a hand watch).

The synthesized TPUs contained up to 85% bio-carbon content. The calculation of bio-carbon content is based on the following formula.

$$\text{Bio-carbon content (\%)} = \frac{\text{Weight of bio-based carbon in grams}}{\text{Weight of total carbon (bio-based and non bio-based) in grams}} \times 100$$

The formation of TPU was confirmed by FTIR spectroscopy. The complete disappearance of the free isocyanate peak at around  $2250\text{ cm}^{-1}$  indicated the formation of TPUs (Figure 2). The peak at  $3319\text{--}3324\text{ cm}^{-1}$  is assigned to the stretching vibration of hydrogen-bonded -NH moieties in the urethane groups of hard segments. In TPUs, C-H stretching vibrations in -CH<sub>2</sub> groups as bimodal bands with maxima were observed in the range of  $2926\text{--}2934\text{ cm}^{-1}$ , respectively. Furthermore, a characteristic band between  $1722\text{--}1730\text{ cm}^{-1}$  and  $1682\text{ cm}^{-1}$  is associated with the stretching vibration of C=O in TPUs; such an observation was reported in the literature for thermoplastic polyurethanes [22]. The bands at  $1535\text{--}1539\text{ cm}^{-1}$  were assigned to stretching vibration of -CN. The peak at  $1722\text{--}1730\text{ cm}^{-1}$  corresponds to the free carbonyl group, whereas the peak at  $1682\text{ cm}^{-1}$  is attributed to the hydrogen-bonded carbonyl group. In TPUs, the bending vibrations of -CH groups were registered between  $1461$  and  $1465\text{ cm}^{-1}$ . TPUs showed multiple IR bands in the range  $1100\text{--}1200\text{ cm}^{-1}$ , related to the C(O)-O-C stretching vibration from the ester groups of polyester polyols.

Furthermore, the structural identity of TPUs was ascertained from <sup>1</sup>H and <sup>13</sup>C NMR. In <sup>1</sup>H NMR, the chemical shift of  $\delta$  6.99–7.07 ppm corresponds to urethane protons (-NHCO-), indicating the formation of TPUs (Figures 3–5). All other backbone protons match with their respective chemical shifts. For example, the signal at around  $\delta$  0.87–0.88 ppm originates from branched methyl protons in TPU2, whereas in the case of TPU3, the peak at  $\delta$  0.83 ppm corresponds to branched methyl protons due to the 3MPDO diol. A clear observation was made from <sup>13</sup>C NMR; the chemical shift at around  $\delta$  157 ppm further suggests the formation of urethane linkage (-NHCO-) due to the reaction of polyol mixture and isocyanate (Figures S8 and S10 for TPU1 and TP2, respectively). The formation of high-molecular-weight TPUs was also confirmed with the help of gel permeation chromatography (GPC). The TPUs displayed a weight average molecular weight ( $M_w$ ) of between  $138 \times 10^3$  and

$179 \times 10^3$  g/mol, and a polydispersity index (PDI) in the range of 2.82–3.36 confirmed the broad distribution of polymeric chains.

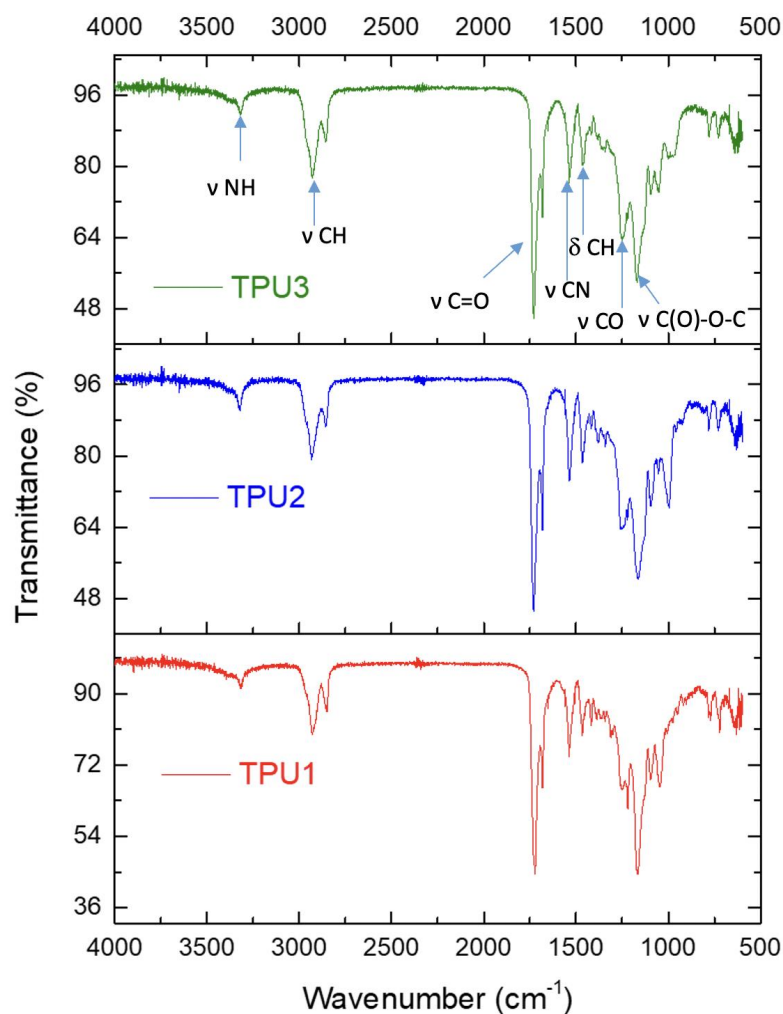


Figure 2. FTIR spectra for TPUs.

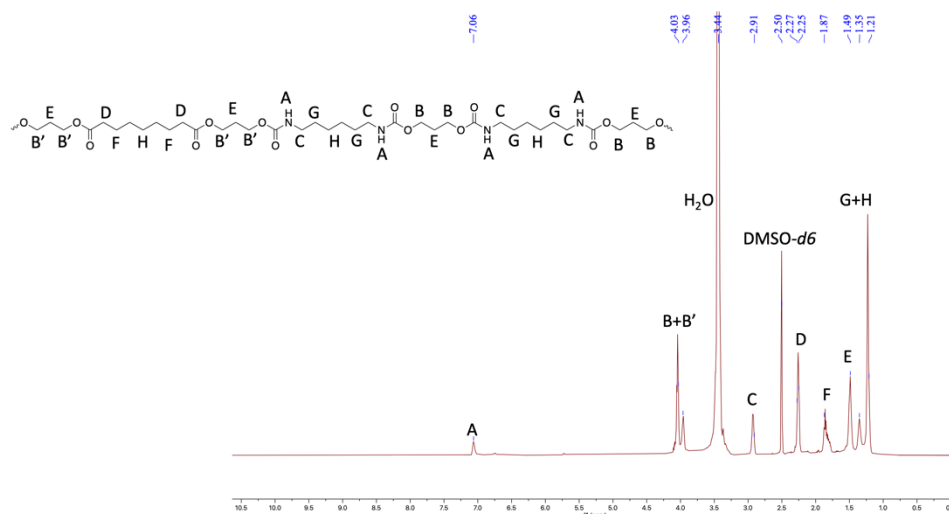
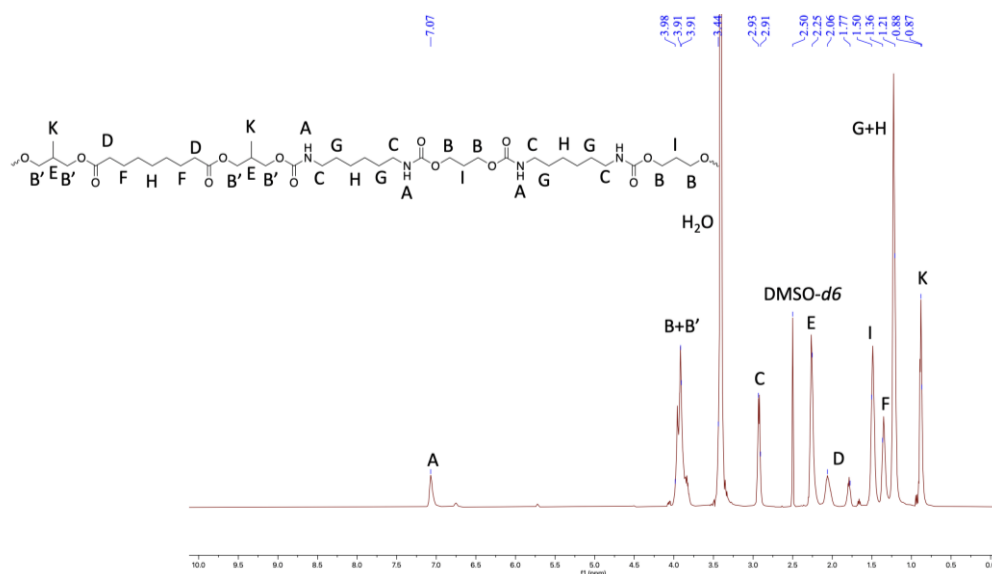
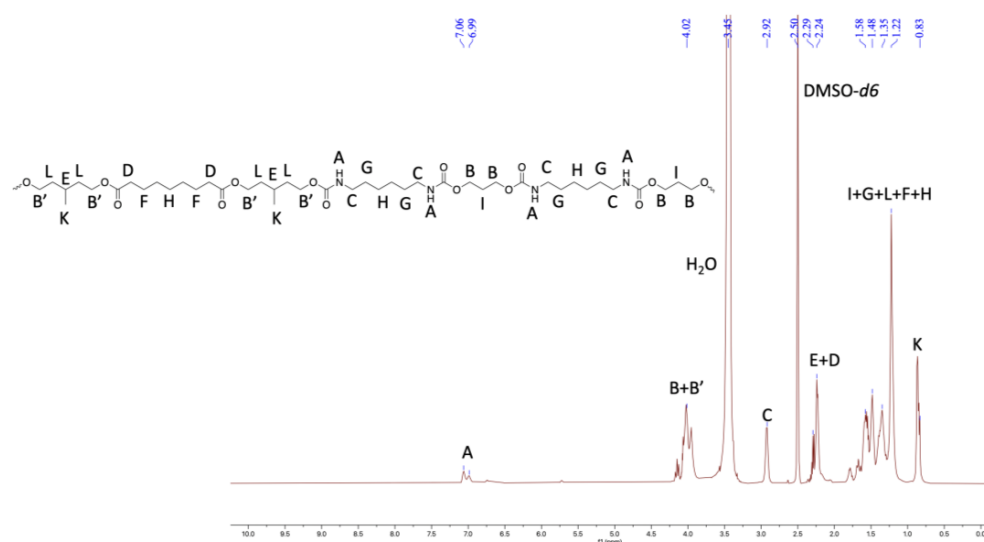


Figure 3.  $^1\text{H}$ NMR of TPU1 in  $\text{DMSO-}d_6$  (500 MHz, 298 K).





**Figure 4.**  $^1\text{H}$ NMR of TPU2 in  $\text{DMSO-}d_6$  (500 MHz, 298 K).



**Figure 5.**  $^1\text{H}$ NMR of TPU3 in  $\text{DMSO-}d_6$  (500 MHz, 298 K).

### 2.3. Properties of Thermoplastic Polyurethanes

Thermal properties of TPUs were evaluated using differential scanning calorimetry (DSC) and thermal gravimetric analysis (TGA). DSC analysis of TPUs was carried out between  $-120\text{ }^\circ\text{C}$  and  $220\text{ }^\circ\text{C}$  under a nitrogen atmosphere. All TPUs displayed clear glass transition temperature values ( $T_g$ s) in low-temperature regions ( $-65\text{ }^\circ\text{C}$  to  $-53\text{ }^\circ\text{C}$ ), which are related to the azelate polyester polyols soft domains (Figure 6). The  $T_g$  values were observed in the order of  $\text{TPU1} > \text{TPU2} > \text{TPU3}$ , with the lower  $T_g$  value associated with a chain length of polyols in TPUs. For example, longer chain length AzA3MPDO polyol-based TPU3 showed a lower  $T_g$  of  $-65\text{ }^\circ\text{C}$  than shorter chain length TPU1 ( $T_g = -53\text{ }^\circ\text{C}$ ; based on AzAPDO polyol). Comparatively, the higher  $T_g$  in the shorter chain length polyol is presumably because of increased hydrogen bonding between azelate polyol soft segments and hard segments (1,3-PDO- and 6HDI-based urethane linkage), which basically decreased the mobility of the azelate polyol chains in TPU1 and TPU2 compared to TPU3. Interestingly, TPU1 made from AzAPDO polyol displayed two melting temperatures,  $T_{m1}$  and  $T_{m2}$ , at  $45\text{ }^\circ\text{C}$  and  $105\text{ }^\circ\text{C}$ , respectively. However, a sharp  $T_m$  was observed at  $45\text{ }^\circ\text{C}$ , which stems from the AzAPDO crystalline soft segments, and  $T_m$  at  $103\text{ }^\circ\text{C}$  is because of

the hard segment, whereas the amorphous TPUs, TPU1, and TPU2, displayed  $T_m$  of 105 °C and 104 °C, respectively. The crystallization temperature ( $T_c$ ) was also observed for TPUs. TPU1 based on AzAPDO polyols showed two distinct crystallization temperatures,  $T_{c1}$  and  $T_{c2}$ , at 19.1 °C and 70.7 °C, respectively, whereas TPU2 displayed  $T_c$  at 38.2 °C and TPU3 displayed  $T_c$  at 54.8 °C. The crystalline TPU1 displayed a higher shore A hardness compared to amorphous TPUs due to the branching structure of TPU2 and TPU3 (Table 4). The hardness of our TPUs entirely depends on the microphase separation of TPUs due to diverse polyols structures; in the case of TPU1, the microphase separation results in higher hardness compared to TPU2 and TPU3, which have lower microphase separation. A similar observation was made in other studies, whereby crystalline azelate polyols were found to be harder than amorphous ones [17].

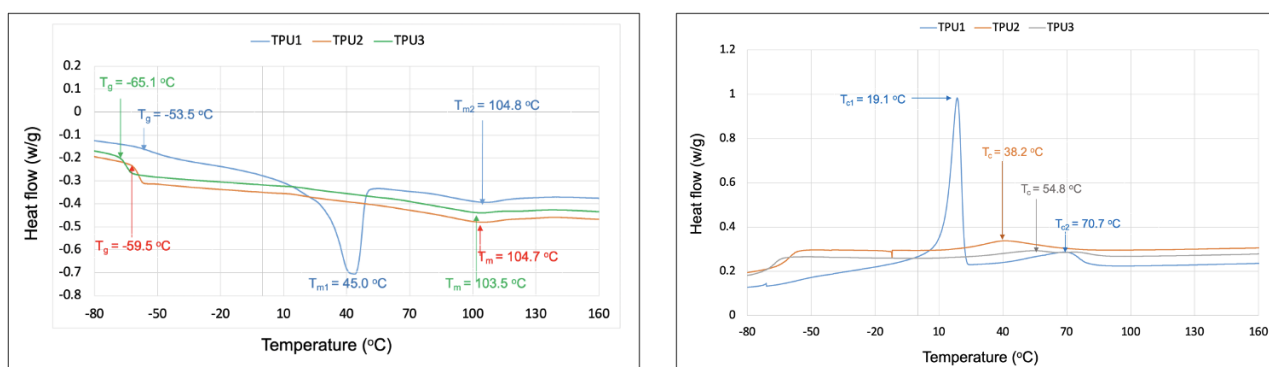


**Figure 6.** DSC analysis of TPUs in nitrogen atmosphere, data recorded from second heating cycle (left) and cooling scan (right).

**Table 4.** Properties of thermoplastic polyurethanes.

Properties	TPU1	TPU2	TPU3
GPC $M_n$ (g/mol)	$55 \times 10^3$	$41 \times 10^3$	$63 \times 10^3$
GPC $M_w$ (g/mol)	$171 \times 10^3$	$138 \times 10^3$	$179 \times 10^3$
GPC $M_w/M_n$	3.11	3.36	2.82
(a) Tensile strength at RT, MPa	48	31	17
(a) Elongation at break at RT, %	765	881	809
Shore A hardness at RT	96	85	82
Thermal transitions (DSC, °C)	$T_g = -53.5$ °C $T_{m1} = 45$ °C $T_{m2} = 104.8$ °C	$T_g = -59.5$ °C $T_m = 104.7$ °C	$T_g = -65.1$ °C $T_m = 103.5$ °C

(a) Tensile strength and percent elongation at break values are the averages of three specimens except for TPU1, which is two specimens.

In TGA analysis, all prepared TPUs showed thermal stability up to 280 °C. Thermal decomposition was observed above this (Figure 7A). The TPU1 and TPU2 showed 29% weight loss at the temperature of 376 °C and 386 °C, respectively, whereas maximum weight loss of around 38% was observed for TPU3 at just 378 °C, confirming the weaker physical interactions of polymer chains in TPU3. DTG curves showed a thermal decomposition at 316 °C, 330 °C, and 336 °C corresponding to the urethane group, and thermal decomposition at 410 °C, 412 °C, and 422 °C originating from ester linkage breakdown at elevated temperatures. The shoulder peak was also observed in the range of 460–465 °C associated with hydrocarbon chain decompositions (Figure 7B). Such thermal decomposition for functional polyurethanes was reported in the literature [23]. Mechanical properties were examined using a dynamic mechanical analyzer (DMA) and universal testing machine (UTM). DMA analysis of TPU1 showed a gradual decrease in storage modulus because of the crystalline nature of the resultant TPU1, which provides more strength in TPU1 compared to TPU2 and TPU3 (Figure 8A). On the other hand, a sharp decrease in storage



modulus was noted for amorphous TPU2 and TPU3. Figure 8B represents the DMA data obtained from tan delta versus temperature curves. The  $T_g$  obtained from the DMA curves for TPUs showed a value in the range of  $-33.2$  to  $-43.8$  °C, which correlated with  $T_g$  values obtained from DSC measurement. The lower  $T_g$  values by DMA analysis further suggest that the TPU possesses soft block structures due to polyols. The TPU1 was found to dissipate less energy due to its crystalline nature. On the other hand, the increasing tan delta in TPU2 and TPU3 (due to their amorphous and more elastic nature) indicates that the material has more energy dissipation potential, so the greater the tan delta, the more dissipative the material at a given applied oscillatory force. The DMA analysis observation was supported by tensile strength measurements. The crystalline TPU1 exhibited the highest tensile strength (48 MPa), which correlated to strong hydrogen bonding or physical interactions between the polymeric chains. In contrast, the amorphous TPUs have a disrupted packing between the polymeric chains due to the presence of a side methyl group (Table 3). Moreover, lower tensile properties for amorphous/branched TPUs are related to the decrease in the degree of microphase separation [18]. After TPU1 (48 MPa), TPU2 was found to have the next-highest tensile strength (31 MPa), and TPU3 was the lowest (18 MPa) (see the stress–strain curve for more details, Figure 9). This is most likely due to the longer chain length structure of TPU3 exhibiting weaker hydrogen bonding between the polymeric chains, resulting in the lower tensile strength value. The crystalline TPU1 had a lower elongation at the break in contrast to the amorphous TPUs. This is due to the presence of a side methyl group in amorphous azelate polyols, resulting in the disruption of crystallization of the soft segment chains [24].

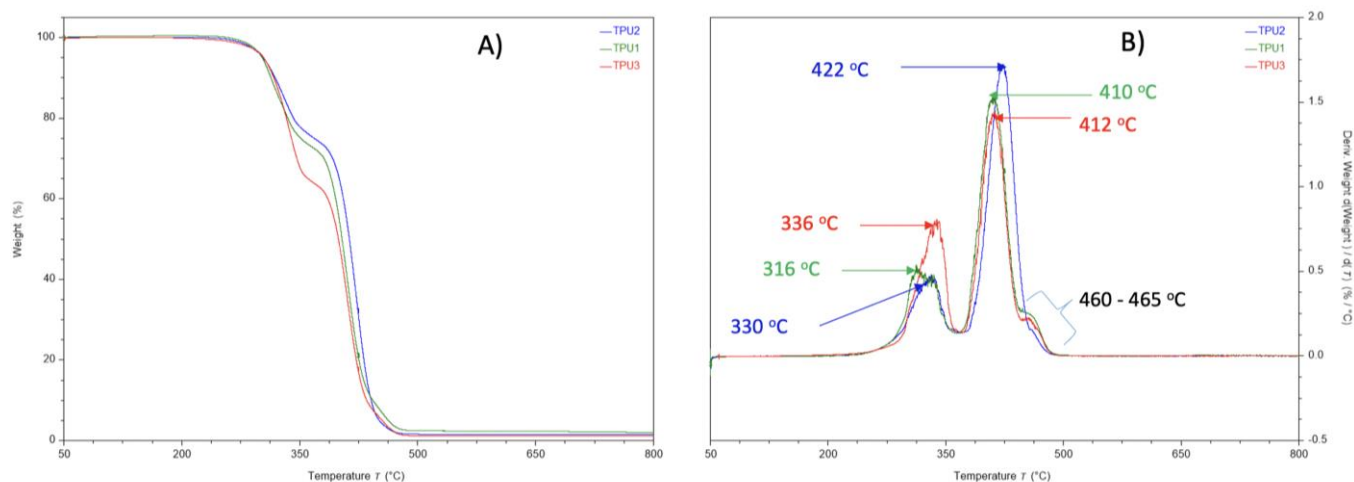


Figure 7. (A) TGA analysis and (B) DTG curve of TPUs under nitrogen atmosphere.

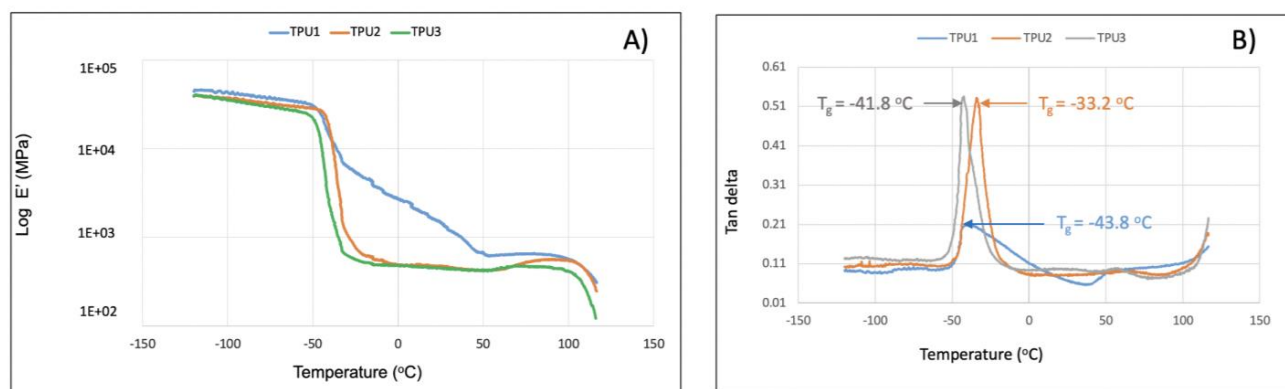


Figure 8. The storage modulus ( $E'$ ) (A) and tangent delta ( $\tan \delta$ ) (B) as a function of temperature for TPUs determined by DMA analysis.

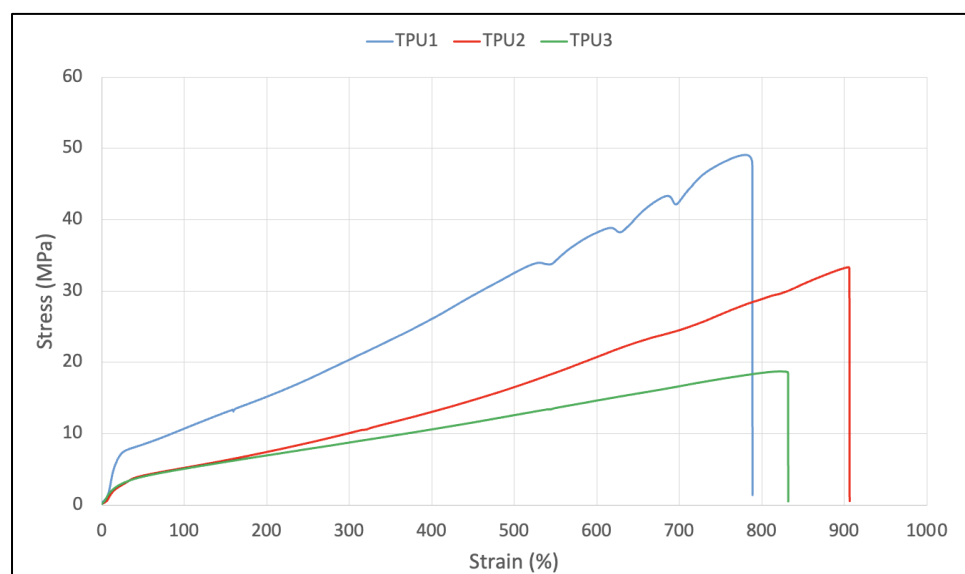


Figure 9. Stress–strain curve for TPUs.

### 3. Materials and Methods

#### 3.1. Materials

Azelaic acid (Crodaacid DC1195, 100% bio-based) with 95% purity was supplied by Croda Inc. The 1,3-propanediol (bio-based) was obtained from Susterra and used as received for polyol and TPU preparations. The 2-methyl 1, 3-propanediol was received from Sigma Aldrich and used without further purifications. The bio-based 3-methyl 1, 5-pentanediol was obtained from Visolis as a gift sample and used as such without purifications. The dibutyltin dilaurate catalyst (DBTDL, 95%) was purchased from Sigma-Aldrich and used without purification. Hexamethylene diisocyanate (6HDI, 98%) was supplied by Alfa Aesar and used without purification for TPU synthesis. Sigma-Aldrich supplied 1.0 M tetrabutylammonium hydroxide in methanol and *p*-toluenesulfonyl isocyanate (96%) for hydroxyl number and acid number titration. HPLC grade toluene, 2-propanol acetonitrile, reagent grade 1-octanol, and potassium hydroxide were supplied by Fisher Chemical for hydroxyl and acid number analysis.

#### 3.2. Measurements

FTIR analysis was carried out on a Perkin Elmer Spectrum X fitted with a ZnSe 1 mm ATR cell. Sixteen scans were taken at  $1.0\text{ cm}^{-1}$  resolution. Proton NMR and carbon NMR spectra were recorded on a JOEL ECA 500. Dynamic mechanical analyzer (DMA) measurement for TPUs was performed out on a TA instrument with a DMA oscillatory temperature ramp using a 3-point bending clamp in the temperature range of  $-120$  to  $120\text{ }^{\circ}\text{C}$ . The hydroxyl number and acid number titrations were carried out according to ASTM 1899 and D664, respectively. Viscosity measurement for polyols was carried out at  $70\text{ }^{\circ}\text{C}$  using a discovery hybrid rheometer 30 (HR 30) instrument. For tensile strength and elongation at break measurement, a universal testing machine (UTM) machine, AGS-X 20KN, was used at the rate of  $100\text{ mm/min}$ . Differential scanning calorimetry (DSC) analysis was performed on a TA instrument from  $-120\text{ }^{\circ}\text{C}$  to  $220\text{ }^{\circ}\text{C}$  at the rate of  $10\text{ }^{\circ}\text{C/min}$  under a nitrogen atmosphere. Thermal gravimetric analysis (TGA) was carried out on TA instrument from  $50\text{ }^{\circ}\text{C}$  to  $900\text{ }^{\circ}\text{C}$  using a temperature ramp of  $10\text{ }^{\circ}\text{C/min}$  in a nitrogen atmosphere. The gel permeation chromatography (GPC) technique is used to calculate the molecular weight and molecular weight distribution (polydispersity index) of the polymers. The molecular weight of TPUs was determined relative to a polystyrene standard and DMF served as the polymer solvent. The flow rate for GPC is  $0.35\text{ mL/min}$  and the temperature is  $60\text{ }^{\circ}\text{C}$ .

### 3.3. Synthesis Method for Polyester Polyols

Polyester polyol synthesis was carried out in a three-necked round bottom glass reactor equipped with a Dean–Stark apparatus, reflux condenser, and an oil bath on a hot plate. Then, under a nitrogen atmosphere, calculated amounts of diacids and diols were added to the reactor (see Table 1 for detailed polyol formulation). The polyester polyol synthesis was started at 150–160 °C and the temperature increased up to 180 °C over a period of 1 h. However, a rapid release of water by-product was observed in the initial 4–5 h. Afterwards, the DBTDL catalyst was added when about 80% water was collected, and the reaction was run until the desired acid and OH number (reactions took approximately 2–3 days) were achieved. The progress of the polyester polyol reactions was monitored by analyzing the acid and hydroxyl numbers in a regular interval of time.

### 3.4. Synthesis Method for TPUs

Polyester polyols and 1,3-propanediol were dried in a vacuum oven for 24 h before polymerization. Then, polyester polyols, 1,3-propane diol as a chain-extender, and catalyst (DBTDL) were weighed into a plastic cup and heated to 75 °C, and the polyol mixture was mixed using the speed mixer (FlackTek, DAC 150.1 FVZ-K) at 2000 rpm. The preheated hexamethylene diisocyanate (6HDI) at 75 °C was then added into the polyol mixture and speed mixed at 2000 rpm for about 1 min. Afterward, the reaction mixture was poured into a Teflon petri dish before a gel point and subsequently cured at 75 °C for 2 days to obtain a desired TPU sheet. Thermal and mechanical properties were performed after one week of room temperature curing. For tensile testing, a dog bone-shaped cutting die was used following the ASTM D638 standard to make sample specimens.

## 4. Conclusions

Here, we report new high bio-carbon content TPUs from both crystalline and amorphous azelate polyester polyols. The synthesized polyester polyols were characterized by proton and carbon NMR spectroscopy. Prepared polyester polyols showed low viscosity behavior at 70 °C, which allowed us to process TPU synthesis at lower temperatures. The TPUs were molded into simple prototypes, i.e., cups and watch bands. The formation of TPUs was ascertained from FTIR analysis, which clearly showed the complete disappearance of the isocyanate peak around 2250 cm<sup>-1</sup>. Proton and carbon NMR analysis also revealed the formation of TPUs. All prepared TPUs displayed adequate thermal and mechanical properties. The TPU synthesized from crystalline azelate polyester polyol was found to be the mechanically strongest and toughest material compared to the TPUs derived from amorphous polyols, as confirmed by tensile strength and storage modulus analysis. These TPUs could be promising candidates for a real-world applications, where the properties and end-of-life scenarios are carefully tuned for use and disposal. These TPUs can be used in the application of making watch bands, mobile case covers, toys, industrial belts, etc. It is through the careful study of renewable materials such as these, and their demonstration as prototypes, that environmentally friendly plastics can find real-world applications.

**Supplementary Materials:** The following supporting information can be downloaded at: <https://www.mdpi.com/article/10.3390/molecules27154885/s1>, Figure S1: <sup>1</sup>H NMR of AzAPDO polyester polyol in CDCl<sub>3</sub> (500 MHz, 298 K); Figure S2: <sup>13</sup>C NMR of AzAPDO polyester polyol in CDCl<sub>3</sub> (125 MHz, 298 K); Figure S3: <sup>1</sup>H NMR of AzA2MPDO polyester polyol in CDCl<sub>3</sub> (500 MHz, 298 K); Figure S4: <sup>13</sup>C NMR of AzA2MPDO polyester polyol in CDCl<sub>3</sub> (125 MHz, 298 K); Figure S5: <sup>1</sup>H NMR of AzA3MPDO polyester polyol in CDCl<sub>3</sub> (500 MHz, 298 K); Figure S6: <sup>13</sup>C NMR of AzA3MPDO polyester polyol in CDCl<sub>3</sub> (125 MHz, 298 K); Figure S7: <sup>1</sup>H NMR of TPU1 in DMSO-*d*<sub>6</sub> (500 MHz, 298 K); Figure S8: <sup>13</sup>C NMR of TPU1 in DMSO-*d*<sub>6</sub> (125 MHz, 298 K); Figure S9: <sup>1</sup>H NMR of TPU2 in DMSO-*d*<sub>6</sub> (500 MHz, 298 K); Figure S10: <sup>13</sup>C NMR of TPU2 in DMSO-*d*<sub>6</sub> (125 MHz, 298 K); Figure S11: <sup>1</sup>H NMR of TPU3 in DMSO-*d*<sub>6</sub> (500 MHz, 298 K).

**Author Contributions:** B.S.R.: Conceptualization, synthesis, chemical and structural research, methodology, investigation, writing—original draft; T.A.P.H.: writing—review and editing, investigation; M.D.B.: writing—review and editing, supervision, project administration. All authors have read and agreed to the published version of the manuscript.

**Funding:** This work was supported by funding from DOE DE-EE0008246 and DE-EE0009295.

**Institutional Review Board Statement:** Not applicable.

**Informed Consent Statement:** Not applicable.

**Data Availability Statement:** The data presented in this study are available on request from the corresponding author.

**Acknowledgments:** The authors are thankful to Algenesis for providing the support and infrastructure to carry out research. The authors thanks Gordon B. Scofield for tensile testing measurements and Anthony Mrse for assistance with the analysis of NMR. The authors also thank Rachel Behrens and Amanda Strom from Material Research Laboratory (MRL), University of California Santa Barbara (UCSB) for assistance with the analysis of DSC, DMA, GPC, and TGA. The MRL shared experimental facilities supported by the MRSEC program of the NSF under award No. DMR 1720256, as a member of the NSF-funded materials research facilities network ([www.mrfn.org](http://www.mrfn.org), accessed on 25 July 2022).

**Conflicts of Interest:** M.D.B. is the founder and holds an equity position in Algenesis Materials, which seeks to commercialize renewable materials.

**Sample Availability:** Samples of compounds are available from the authors after re-synthesis.

## References

1. Tschan, M.J.L.; Brulé, E.; Haquette, P.; Thomas, C.M. Synthesis of Biodegradable Polymers from Renewable Resources. *Polym. Chem.* **2012**, *3*, 836–851. [[CrossRef](#)]
2. Sawpan, M.A. Polyurethanes from Vegetable Oils and Applications: A Review. *J. Polym. Res.* **2018**, *25*, 184. [[CrossRef](#)]
3. Maisonneuve, L.; Chollet, G.; Grau, E.; Cramail, H. Vegetable Oils: A Source of Polyols for Polyurethane Materials. *OCL* **2016**, *23*, D508. [[CrossRef](#)]
4. Rajput, B.S.; Gaikwad, S.R.; Menon, S.K.; Chikkali, S.H. Sustainable Polyacetals from Isohexides. *Green Chem.* **2014**, *16*, 3810. [[CrossRef](#)]
5. Rajput, B.S.; Chander, U.; Arole, K.; Stempfle, F.; Menon, S.; Mecking, S.; Chikkali, S.H. Synthesis of Renewable Copolyacetals with Tunable Degradation. *Macromol. Chem. Phys.* **2016**, *217*, 1396–1410. [[CrossRef](#)]
6. Rajput, B.S.; Ram, F.; Menon, S.K.; Shanmuganathan, K.; Chikkali, S.H. Cross-Metathesis of Biorenewable Dioxalates and Diols to Film-Forming Degradable Polyoxalates. *J. Polym. Sci. Part A Polym. Chem.* **2018**, *56*, 1584–1592. [[CrossRef](#)]
7. Hai, T.A.P.; Tessman, M.; Neelakantan, N.; Samoylov, A.A.; Ito, Y.; Rajput, B.S.; Pourahmady, N.; Burkart, M.D. Renewable Polyurethanes from Sustainable Biological Precursors. *Biomacromolecules* **2021**, *22*, 1770–1794. [[CrossRef](#)]
8. Pandey, S.; Rajput, B.S.; Chikkali, S.H. Refining Plant Oils and Sugars to Platform Chemicals, Monomers, and Polymers. *Green Chem.* **2021**, *23*, 4255–4295. [[CrossRef](#)]
9. Rosenboom, J.G.; Langer, R.; Traverso, G. Bioplastics for a Circular Economy. *Nat. Rev. Mater.* **2022**, *7*, 117–137. [[CrossRef](#)] [[PubMed](#)]
10. Gandini, A.; Lacerda, T.M.; Carvalho, A.J.F.; Trovatti, E. Progress of Polymers from Renewable Resources: Furans, Vegetable Oils, and Polysaccharides. *Chem. Rev.* **2016**, *116*, 1637–1669. [[CrossRef](#)] [[PubMed](#)]
11. Hasan, M.M.F.; Rossi, L.M.; Debecker, D.P.; Leonard, K.C.; Li, Z.; Makhubela, B.C.E.; Zhao, C.; Kleij, A. Can CO<sub>2</sub> and Renewable Carbon Be Primary Resources for Sustainable Fuels and Chemicals? *ACS Sustain. Chem. Eng.* **2021**, *9*, 12427–12430. [[CrossRef](#)]
12. Datta, J.; Kasprzyk, P. Thermoplastic Polyurethanes Derived from Petrochemical or Renewable Resources: A Comprehensive Review. *Polym. Eng. Sci.* **2018**, *58*, E14–E35. [[CrossRef](#)]
13. Tharcis, M.; Badel, T.; Jéol, S.; Fleury, E.; Méchin, F. High Elongation Thermoplastic Polyester-Urethanes Based on Widely Available Diacid Intermediates. *J. Appl. Polym. Sci.* **2016**, *133*, 1–15. [[CrossRef](#)]
14. Wan, Y.; Lee, J.M. Toward Value-Added Dicarboxylic Acids from Biomass Derivatives via Thermocatalytic Conversion. *ACS Catal.* **2021**, *11*, 2524–2560. [[CrossRef](#)]
15. Sonnenschein, M.F.; Guillaudeu, S.J.; Landes, B.G.; Wendt, B.L. Comparison of Adipate and Succinate Polyesters in Thermoplastic Polyurethanes. *Polymer* **2010**, *51*, 3685–3692. [[CrossRef](#)]
16. Mohd Noor, N.; Sendijarevic, A.; Sendijarevic, V.; Sendijarevic, I.; Tuan Ismail, T.N.M.; Mohd Noor, M.A.; Shoot Kian, Y.; Abu Hassan, H. Comparison of Adipic Versus Renewable Azelaic Acid Polyester Polyols as Building Blocks in Soft Thermoplastic Polyurethanes. *JAOCS, J. Am. Oil Chem. Soc.* **2016**, *93*, 1529–1540. [[CrossRef](#)]

17. Tuan Ismail, T.N.M.; Ibrahim, N.A.; Sendijarevic, V.; Sendijarevic, I.; Schiffman, C.M.; Hoong, S.S.; Mohd Noor, M.A.; Poo Palam, K.D.; Yeong, S.K.; Idris, Z.; et al. Thermal and Mechanical Properties of Thermoplastic Urethanes Made from Crystalline and Amorphous Azelate Polyols. *J. Appl. Polym. Sci.* **2019**, *136*, 1–11. [[CrossRef](#)]
18. Phung Hai, T.A.; Neelakantan, N.; Tessman, M.; Sherman, S.D.; Griffin, G.; Pomeroy, R.; Mayfield, S.P.; Burkart, M.D. Flexible Polyurethanes, Renewable Fuels, and Flavorings from a Microalgae Oil Waste Stream. *Green Chem.* **2020**, *22*, 3088–3094. [[CrossRef](#)]
19. Tuan Ismail, T.N.M.; Azowa Ibrahim, N.; Sendijarevic, A.; Sendijarevic, I.; Schiffman, C.M.; Hoong, S.S.; Mohd Noor, M.A.; Poo Palam, K.D.; Yeong, S.K.; Idris, Z.; et al. Oscillatory Structure-Property Correlation in Azelate Polyols and Thermoplastic Polyurethanes. *J. Appl. Polym. Sci.* **2018**, *135*, 1–10. [[CrossRef](#)]
20. Tuan Ismail, T.N.M.; Ibrahim, N.A.; Poo Palam, K.D.; Sendijarevic, A.; Sendijarevic, I.; Schiffman, C.M.; Hoong, S.S.; Mohd Noor, M.A.; Yeong, S.K.; Abd. Malek, E.; et al. Improved Dynamic Properties of Thermoplastic Polyurethanes Made from Co-Monomeric Polyester Polyol Soft Segments Based on Azelaic Acid. *J. Appl. Polym. Sci.* **2021**, *138*, 1–14. [[CrossRef](#)]
21. Saralegi, A.; Rueda, L.; Fernández-D'Arilas, B.; Mondragon, I.; Eceiza, A.; Corcuera, M.A. Thermoplastic Polyurethanes from Renewable Resources: Effect of Soft Segment Chemical Structure and Molecular Weight on Morphology and Final Properties. *Polym. Int.* **2013**, *62*, 106–115. [[CrossRef](#)]
22. Parcheta, P.; Głowińska, E.; Datta, J. Effect of Bio-Based Components on the Chemical Structure, Thermal Stability and Mechanical Properties of Green Thermoplastic Polyurethane Elastomers. *Eur. Polym. J.* **2020**, *123*, 109422. [[CrossRef](#)]
23. Siyanbola, T.O.; Sasidhar, K.; Rao, B.V.S.K.; Narayan, R.; Olaofe, O.; Akintayo, E.T.; Raju, K.V.S.N. Development of Functional Polyurethane-ZnO Hybrid Nanocomposite Coatings from Thevetia Peruviana Seed Oil. *J. Am. Oil Chem. Soc.* **2015**, *92*, 267–275. [[CrossRef](#)]
24. Kojio, K.; Furukawa, M.; Nonaka, Y.; Nakamura, S. Control of Mechanical Properties of Thermoplastic Polyurethane Elastomers by Restriction of Crystallization of Soft Segment. *Materials* **2010**, *3*, 5097–5110. [[CrossRef](#)] [[PubMed](#)]